Supplementary Information

Improved Safety of Chimeric Antigen Receptor T Cells Indirectly Targeting Antigens via Switchable Adaptors

Hyung Bae Park[1,2,3], Ki Hyun Kim[1,3], Ju Hwan Kim[4], Sang Il Kim[1,3], Yu Mi Oh[1], Miseung Kang[1,2], Seoho Lee[1,2], Siwon Hwang[1,2], Hyeonmin Lee[1,3], TaeJin Lee[4,5], Seungbin Park[5], Ji Eun Lee[1,3], Ga Ram Jeong[1,6], Dong Hyun Lee[7], Hyewon Youn[3,8], Eun Young Choi[2,9], Woo Chan Son[10], Sang J. Chung[5,*], Junho Chung[1,2,3,*], and Kyungho Choi[1,2,3,*]

[1]Department of Biochemistry and Molecular Biology, [2]Department of Biomedical Sciences, and [3]Cancer Research Institute, Seoul National University College of Medicine, Seoul, Republic of Korea. [4]AbTis Co. Ltd., Suwon, Gyeonggi-do, Republic of Korea. [5]Department of Biopharmaceutical Convergence, School of Pharmacy, Sungkyunkwan University, Suwon, Gyeonggi-do, Republic of Korea. [6]Ticaros Inc., Seoul, Republic of Korea. [7]Department of Medical Science, AMIST, University of Ulsan College of Medicine, Asan Medical Center, Seoul, Republic of Korea. [8]Department of Nuclear Medicine, Cancer Imaging Center, Seoul National University Hospital, Seoul, Republic of Korea. [9]Institute of Human Environment Interface Biology, Seoul National University College of Medicine, Seoul, Republic of Korea. [10]Department of Pathology, University of Ulsan College of Medicine, Asan Medical Center, Seoul, Republic of Korea. [*]These authors jointly supervised this work.

Corresponding authors:
Kyungho Choi, Department of Biochemistry and Molecular Biology, Seoul National University College of Medicine, 103 Daehak-ro, Jongno-gu, Seoul 03080, Republic of Korea.
E-mail: khchoi@snu.ac.kr
or Junho Chung, Department of Biochemistry and Molecular Biology, Seoul National University College of Medicine, 103 Daehak-ro, Jongno-gu, Seoul 03080, Republic of Korea.
E-mail: jjhchung@snu.ac.kr
or Sang J. Chung, Department of Biopharmaceutical Convergence, School of Pharmacy, Sungkyunkwan University, 2066 Seoburo, Jangan-gu, Suwon, Gyeonggido 16419, Republic of Korea
E-mail: sjchung@skku.edu

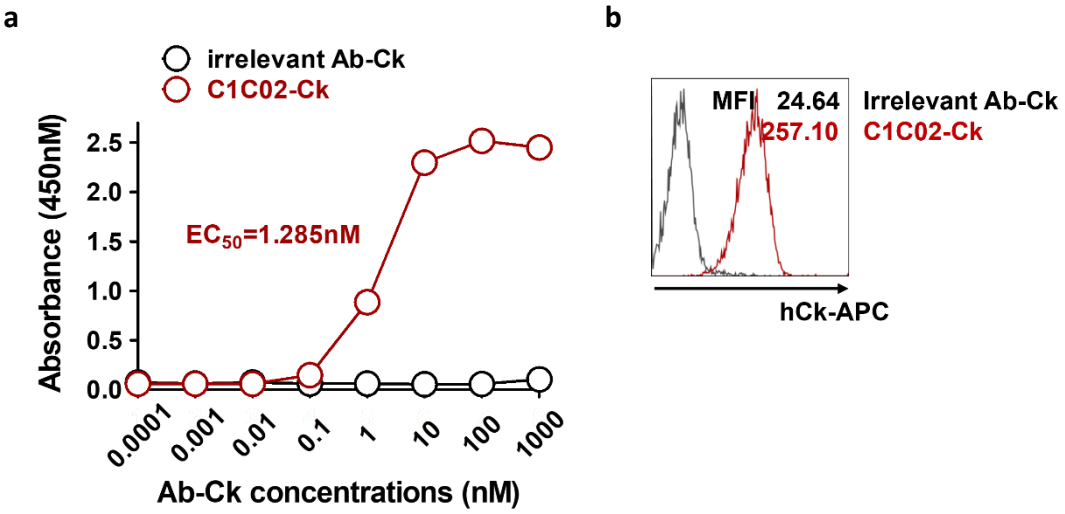

Supplementary Fig. 1 | Anti-mouse CD40 antibody (clone C1C02) binds to both recombinant CD40 protein and cell-surface CD40 on A20 lymphoma cells. a Recombinant mouse CD40-Fc (2.5 μg/ml) was coated on an ELISA plate, and serial dilutions of C1C02-Cκ or irrelevant scFv-Cκ were loaded. Bound scFv-Cκs were detected by secondary anti-human Cκ-HRP followed by chromogenic reaction with TMB substrate, measured in duplicate. Absorbance was measured at 450 nm. The EC_{50} of antibody binding was calculated as the dose that showed 50% of the absorbance of maximal binding. Data are presented as mean ± SEM. Results are representative of two independent experiments. **b** A20, a CD40-expressing mouse B-cell lymphoma cells were stained with C1C02-Cκ or irrelevant scFv-Cκ (1 μg/1×10^5 cells) followed by secondary anti-human Cκ-APC. Binding intensity of the scFv-Cκs was analyzed by flow cytometry. Numbers are mean fluorescence intensities (MFIs) of the binding. Results are representative of three independent experiments. Source data are provided in the Source Data file.

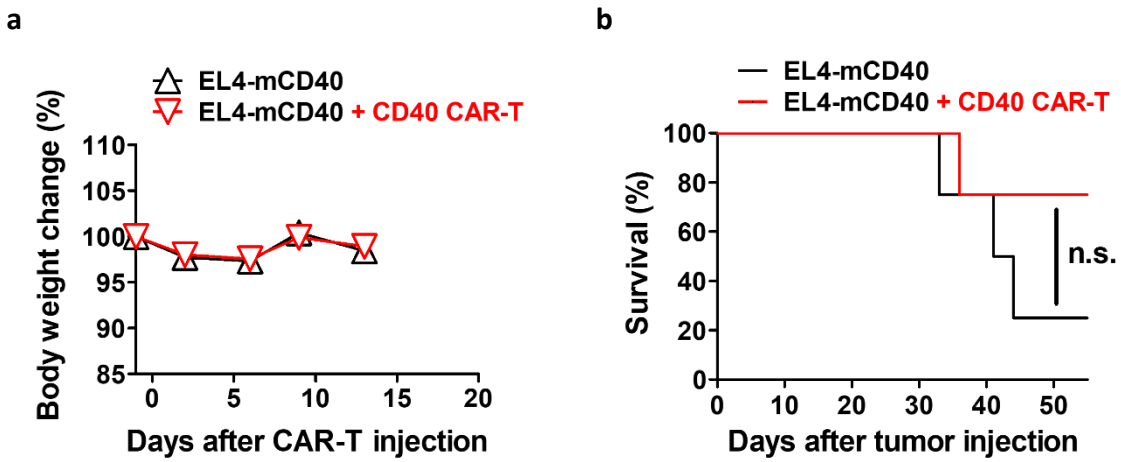

Supplementary Fig. 2 | CD40 CAR-T cells tend to show antitumor efficacy without lethal toxicity in CD40 knockout mice. CD40 knockout B6 mice were injected *i.v.* with mouse CD40-transfected EL4 lymphoma (EL4-mCD40) cells (5×10^5) on day 0, irradiated (3 Gy) for lymphodepletion on day 6, and injected *i.v.* with CD40 CAR-T cells (5×10^6) on day 7. Body weight change (**a**, mean ± SEM) and survival (**b**) were measured (n=4) and analyzed by log-rank (Mantel-Cox) test (**b**, n.s., not significant). Statistical significance could not be reached due to the small number of mice used for each group. Source data are provided in the Source Data file.

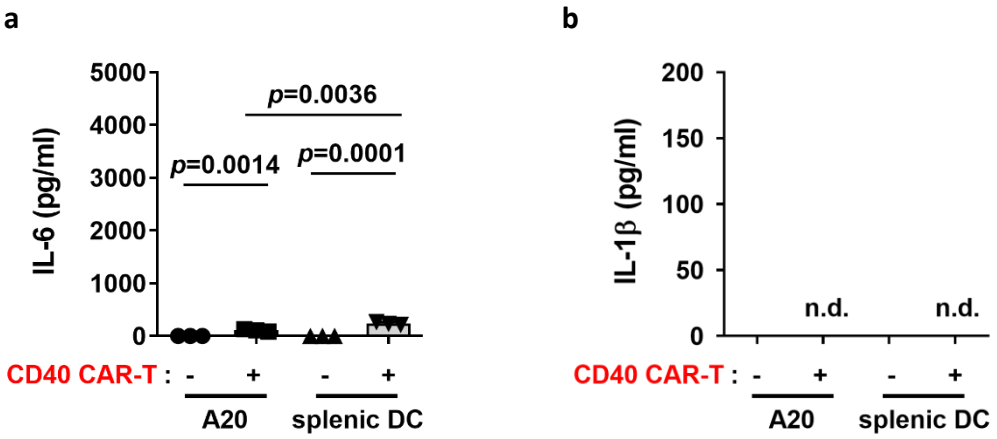

Supplementary Fig. 3 | Splenic dendritic cells produce IL-6 when co-cultured with CD40 CAR-T cells. Production of IL-6 (**a**) or IL-1β (**b**) after co-culture of CD40 CAR-T cells with A20 or splenic dendritic cells for 24 hours, measured in triplicate. Results are representative of three independent experiments. Data are presented as mean ± SEM. Statistical significance was determined by unpaired two-tailed *t*-test. *p*: p-value. n.d.: not detected. Source data are provided in the Source Data file.

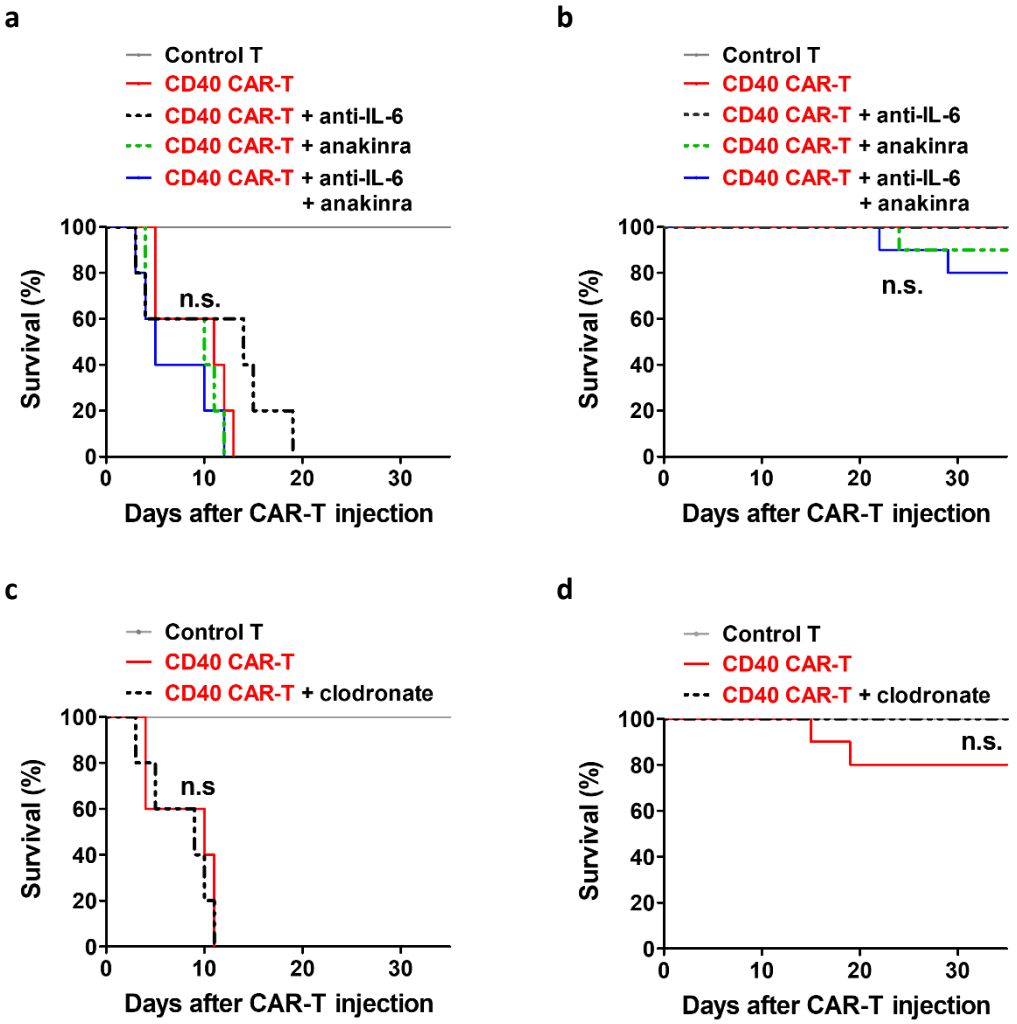

Supplementary Fig. 4 | Neutralization of IL-6 and IL-1β or depletion of macrophages cannot alleviate the lethal toxicity of CD40 CAR-T cells. Balb/C mice were irradiated (2.5 Gy) for lymphodepletion on day -1 and injected with 5×10^6 (**a, c**) or 1×10^6 (**b, d**) control T cells or CD40 CAR-T cells on day 0. IL-6 or IL-1β neutralization (**a, b**) and phagocyte depletion (**c, d**) were performed as described in Methods. Survival was monitored daily and analyzed by log-rank (Mantel-Cox) test (n.s., not significant). Results are representative of two independent experiments (*n*=5) (**a, c**) or pooled from two replicate experiments (*n*=10) (**b, d**). Source data are provided in the Source Data file.

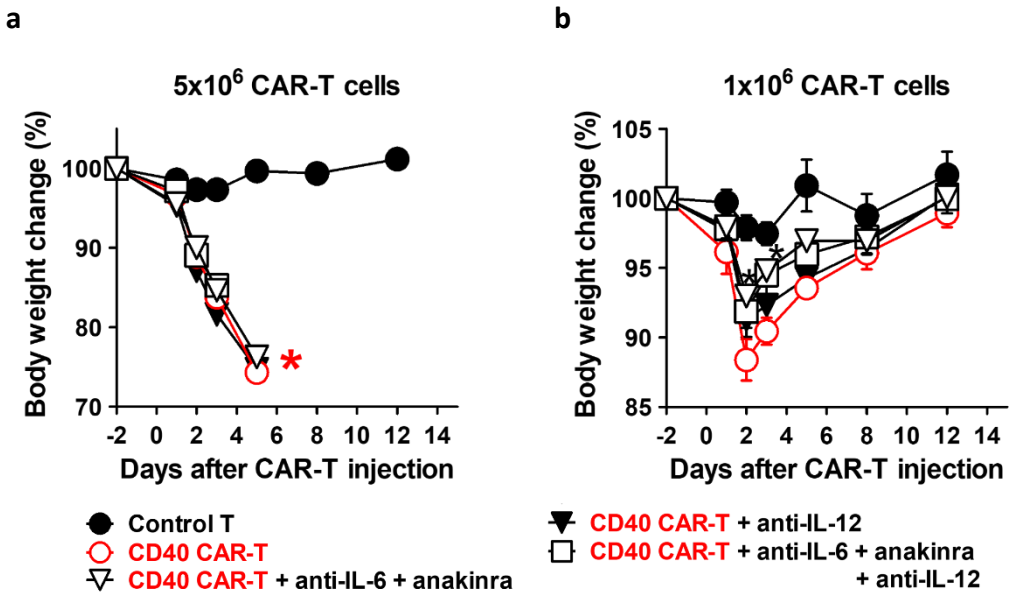

Supplementary Fig. 5 | IL-12 blockade does not facilitate the toxicity-reducing effect of anti-IL-6 and anakinra in CD40 CAR-T cell-treated mice. Balb/C mice were irradiated (2.5 Gy) for lymphodepletion on day -1 and injected with 5×10^6 (**a**) or 1×10^6 (**b**) control T cells or CD40 CAR-T cells on day 0. IL-6, IL-12 or IL-1β neutralization was performed as described in Methods. Body weight changes were measured (n=5). Body weight measurements were halted when mice began to die (red asterisks in **a**). Data are presented as mean ± SEM. and statistical significance was determined by 1-way ANOVA (**b**). *: p=0.0002 on day 2 and p=0.0004 on day 3 for anti-IL-6+anakinra treated group *vs*. CD40 CAR-T group. Results are representative of two independent experiments. p: p-value. Source data are provided in the Source Data file.

Supplementary Fig. 6 | Clodronate treatment effectively eliminates macrophages *in vivo*. Balb/c mice were treated intraperitoneally with clodronate liposomes (1 mg/head) for 3 consecutive days, and peritoneal lavage fluid was collected the next day. Macrophage depletion was confirmed by FACS staining with anti-F4/80.

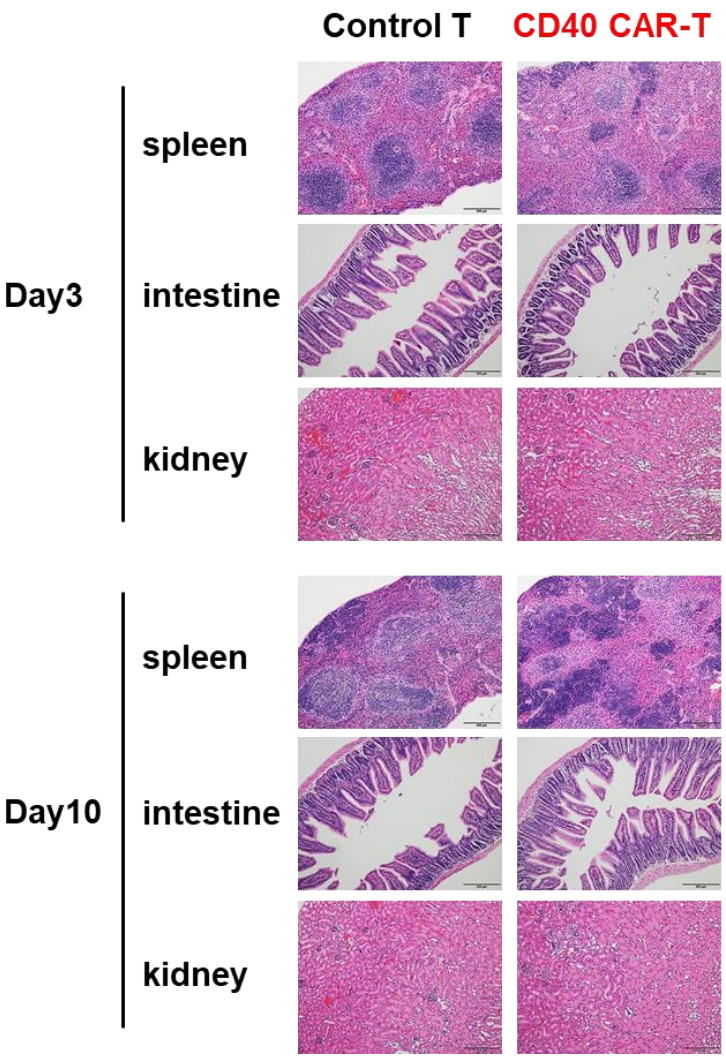

Supplementary Fig. 7 | Histological examination of various organs in CD40 CAR-T cell-treated mice. Balb/C mice were irradiated (2.5 Gy) for lymphodepletion on day -1 and injected with control T cells (5×10^6) or CD40 CAR-T cells (1×10^6) on day 0. Histology of spleen, intestine, and kidney was examined by H&E staining 3 and 10 days after CAR-T cell injection (100× magnification, scale bar: 200 μm). Results are representative of two independent experiments.

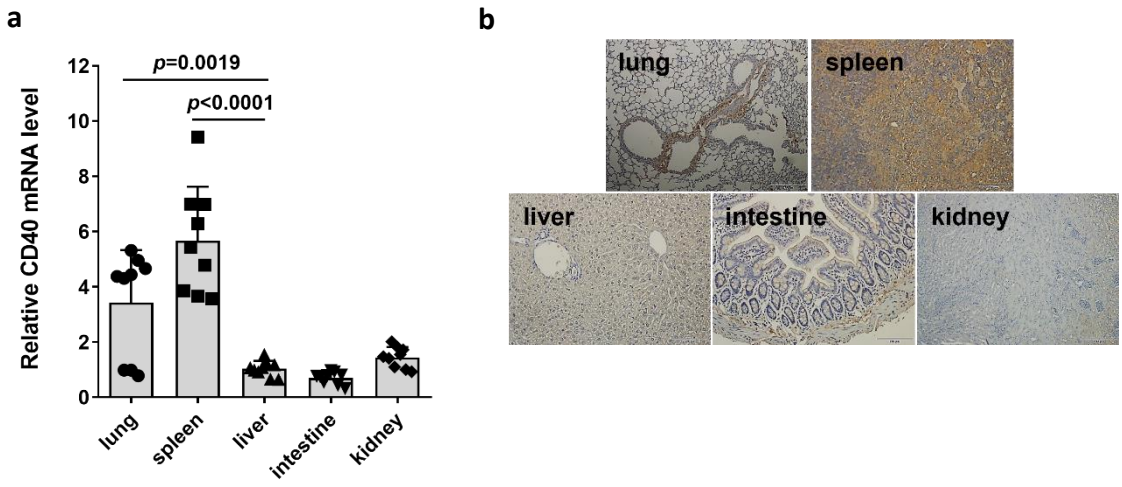

Supplementary Fig. 8 | CD40 is highly expressed in lung and spleen. a Evaluation of CD40 mRNA expression level in mouse tissues. Total RNAs were extracted from various organs (lung, spleen, liver, intestine, and kidney) of normal Balb/C mice and subjected to quantitative RT-PCR of CD40 or β-actin mRNA. CD40 mRNA expression level was determined from the triplicate samples (*n*=3) from each tissue and normalized to that of β-actin. Relative levels were calculated by dividing each value by the average value of liver. The average relative CD40 mRNA levels from the triplicates were plotted. Data are presented as mean ± SEM and statistical significance was determined by unpaired two-tailed *t*-test. *p*: p-value. **b** Evaluation of CD40 protein expression in normal Balb/C mouse tissues by immunohistochemistry using anti-mouse CD40 antibody (C1C02-Cκ). (100× magnification, scale bar: 200 μm). Results are representative of two independent experiments (**a, b**). Source data are provided in the Source Data file.

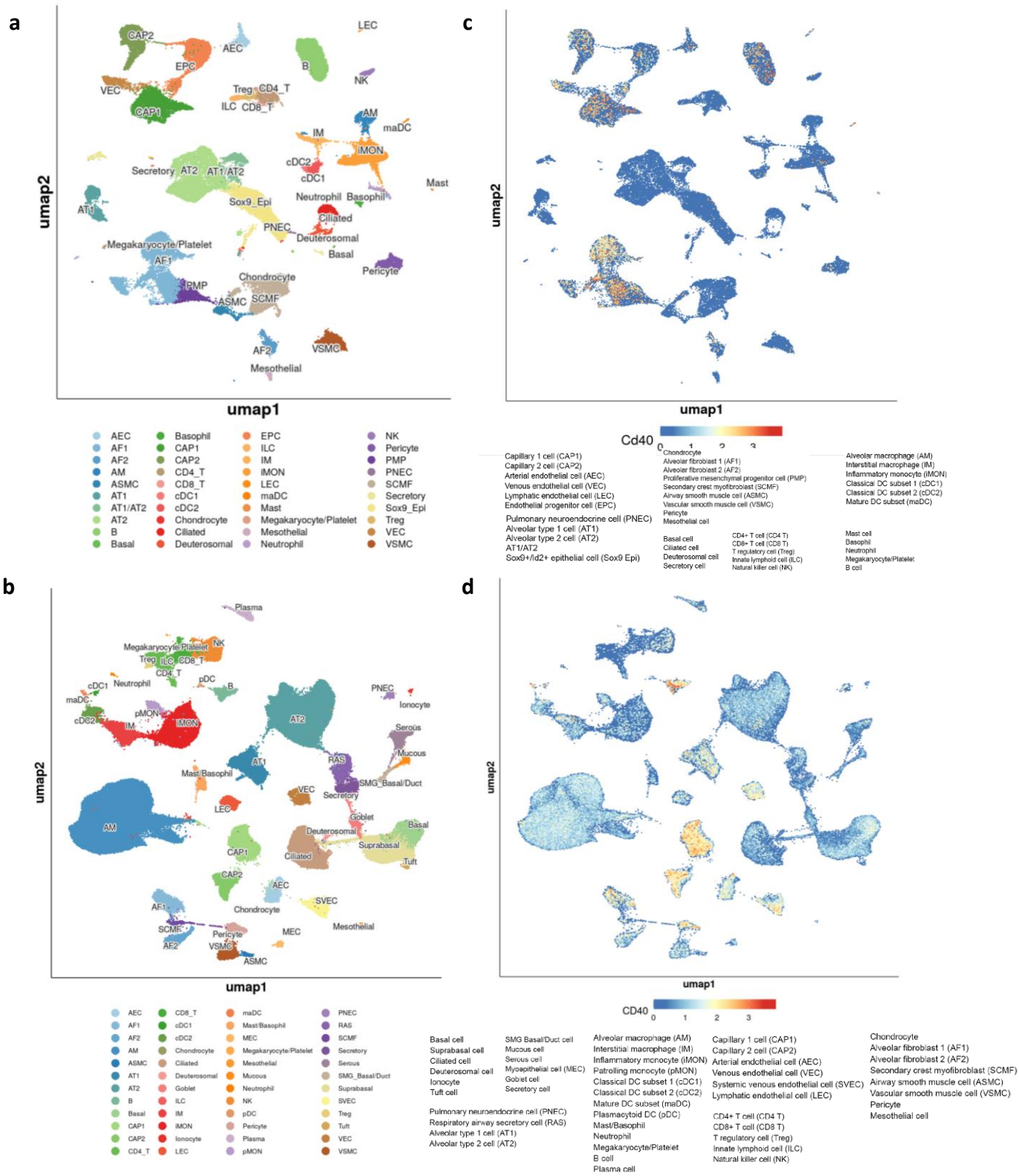

Supplementary Fig. 9 | CD40 is highly expressed on vascular cell types in mouse and human lung. Using a published web-based search tool[63] on the scRNAseq database for mouse (**a**) and human lung (**b**) (https://app.lungmap.net/app/shinycell-mouse-lung-cellref, https://app.lungmap.net/app/shinycell-human-lung-cellref), mouse (**c**) and human (**d**) CD40 mRNA expression was evaluated on various cell types in the lung. Mouse CD40 mRNA is enriched in vascular cell types (capillary1/2, venous endothelial cell, arterial endothelial cell, and endothelial progenitor cell) as well as platelet, alveolar fibroblast and B cell (**c**). Human CD40 mRNA is enriched in vascular cell types (capillary1/2, venous endothelial cell, arterial endothelial cell, systemic venous endothelial cell, and pericyte) as well as alveolar fibroblast and B cell (**d**).

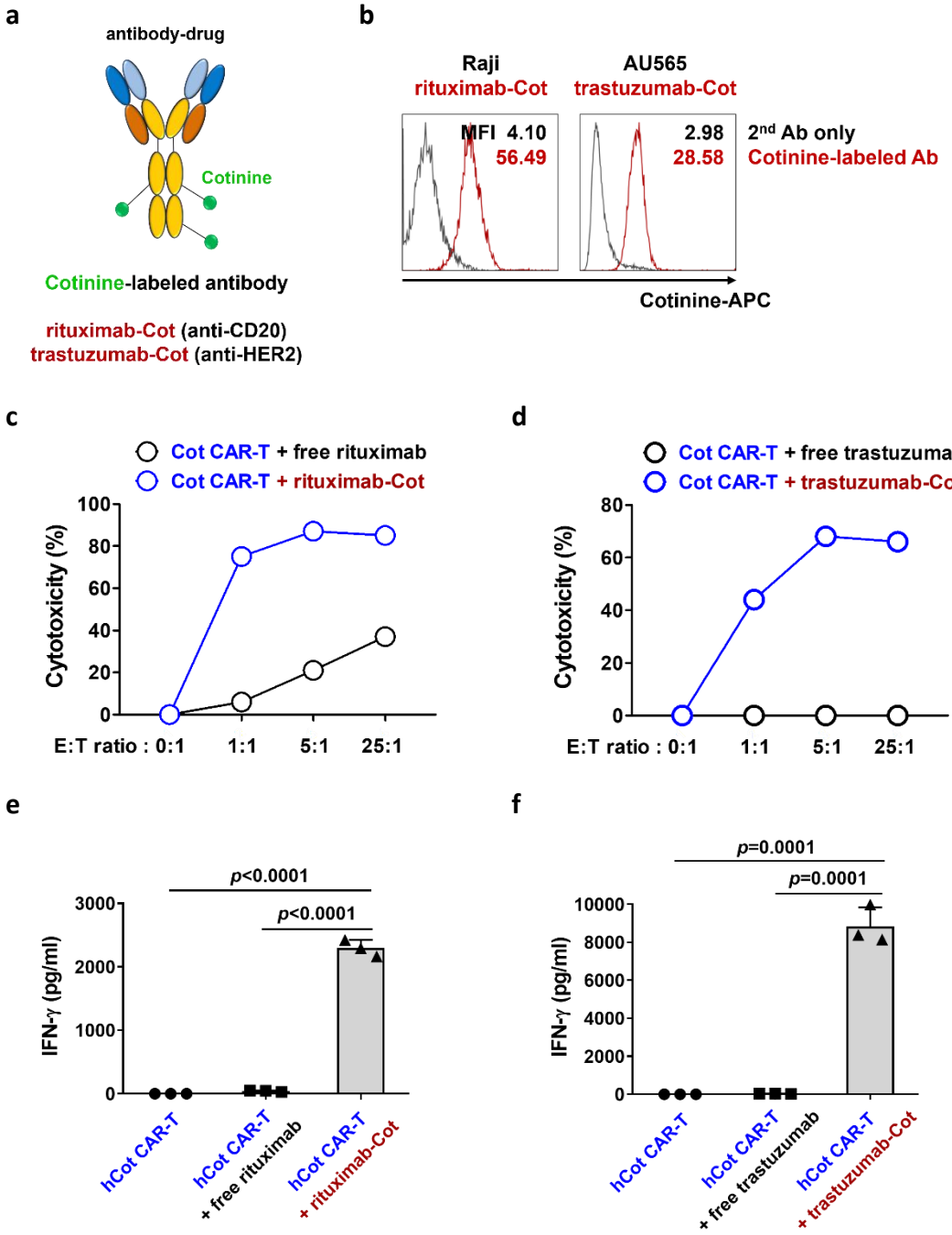

Supplementary Fig. 10 | Verification of the switchable CAR function of Cot CAR-T cells using cotinine-labeled rituximab or trastuzumab. a Schematic diagram of cotinine-labeled antibodies. **b** Flow cytometric verification of binding of cotinine-labeled anti-CD20 antibody (rituximab-Cot) or anti-HER2 antibody (trastuzumab-Cot) to $CD20^+$ tumor cells (Raji) or $HER2^+$ tumor cells (AU565), respectively. **c, d** Verification of anti-tumor cytotoxicity of Cot CAR-T cells with cotinine-labeled antibodies. PKH26-labeled Raji (**c**) or AU565 (**d**) cells (target) were preincubated with free rituximab/rituximab-Cot (**c**) or free trastuzumab/trastuzumab-Cot (**d**) and then co-cultured with Cot CAR-T cells (effector) at the indicated ratios for 6 hours. Percent cytotoxicity was calculated from flow cytometry-based viable cell counting. **e, f** Verification of Cot CAR-T cell activation in the presence of cotinine-labeled antibodies. Raji (**e**) or AU565 (**f**) cells were preincubated with free rituximab/rituximab-Cot (**e**) or free trastuzumab/trastuzumab-Cot (**f**) and then co-cultured with Cot CAR-T cells for 24 hours. The amount of IFN-γ in the culture supernatants was measured in triplicate. Data are presented as mean ± SEM and statistical significance was determined by unpaired two-tailed *t*-test. *p*: p-value. Results are representative of two independent experiments (**c-f**). Source data are provided in the Source Data file.

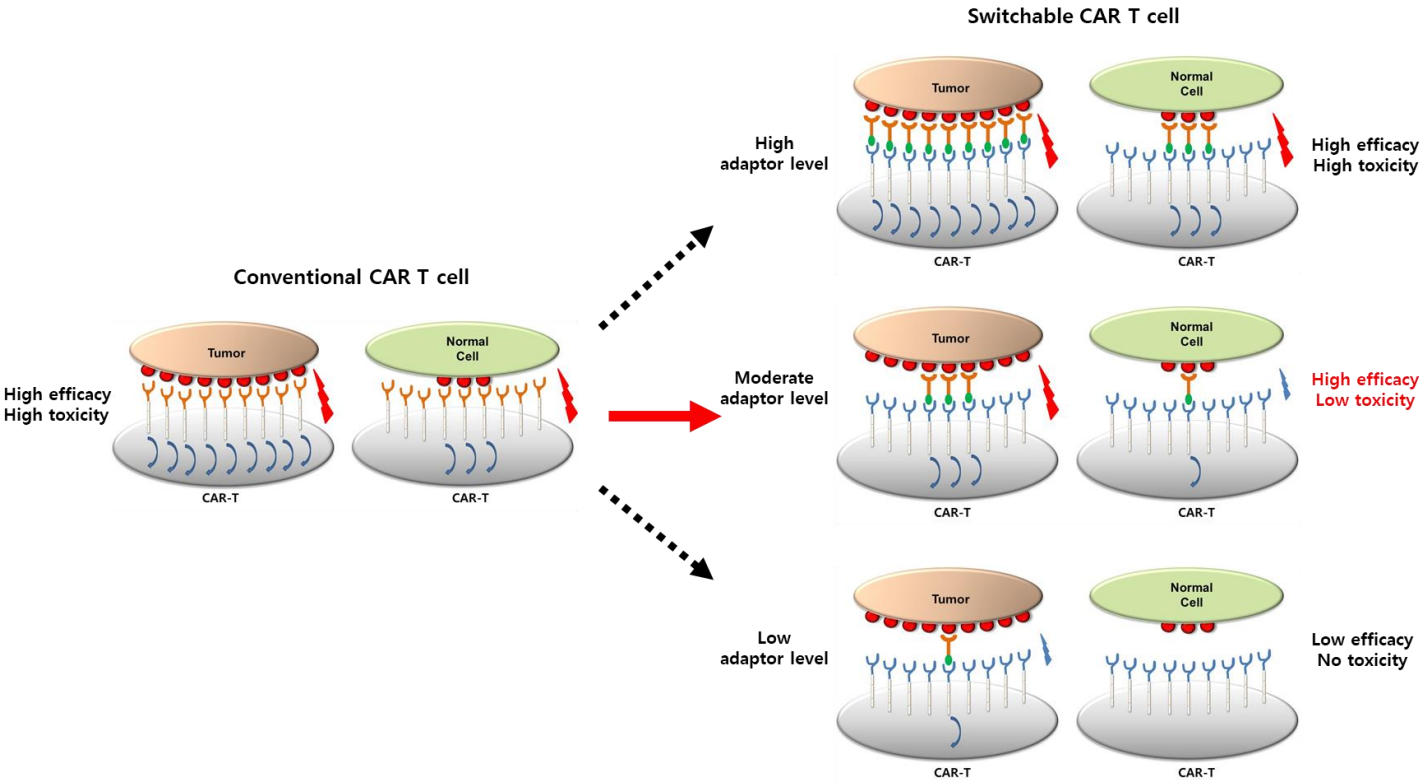

Supplementary Fig. 11 | Schematic representation of toxicity regulation by switchable CAR-T cells. If the engagement of at least 3 CAR molecules is the threshold for CAR-T cell activation, then tumor cells expressing 9 tumor antigens (TAs) and normal cells expressing 3 TAs would similarly activate conventional CAR-T cells, leading to normal cell toxicity (left). For switchable CAR-T cells, if the adaptors are present at a sufficiently high level, the adaptors will bind to all 3 TAs on normal cells, resulting in normal cell toxicity just as with conventional CAR-T cells (top right). However, at a moderate level of the adaptors, which allows the adaptor to bind only 1/3 of the TAs on the cell surface, tumor cells would still have 3 adaptors on the cell surface that can activate CAR-T cells, whereas normal cells would have only 1 adaptor on the cell surface, which is not enough for CAR-T cell activation (middle right). Therefore, at this adaptor level, tumor cells will be killed by CAR-T cells, but normal cells will not, opening a window for efficient tumor killing without normal cell toxicity. At a low adaptor level, which allows the adaptor to bind 1/9 of the TAs on the cell surface, the adaptors will only bind 1 TA on tumor cells, which is insufficient to activate T cells, while not binding normal cells at all. Hence, at this level, neither tumor cell killing nor normal cell killing will occur (lower right). Therefore, this adaptor level will not be appropriate for CAR-T cell efficacy.
Thus, switchable CAR-T cells can have an optimal therapeutic window by adjusting the adaptor levels to moderate ones, while conventional CAR-T cells cannot.

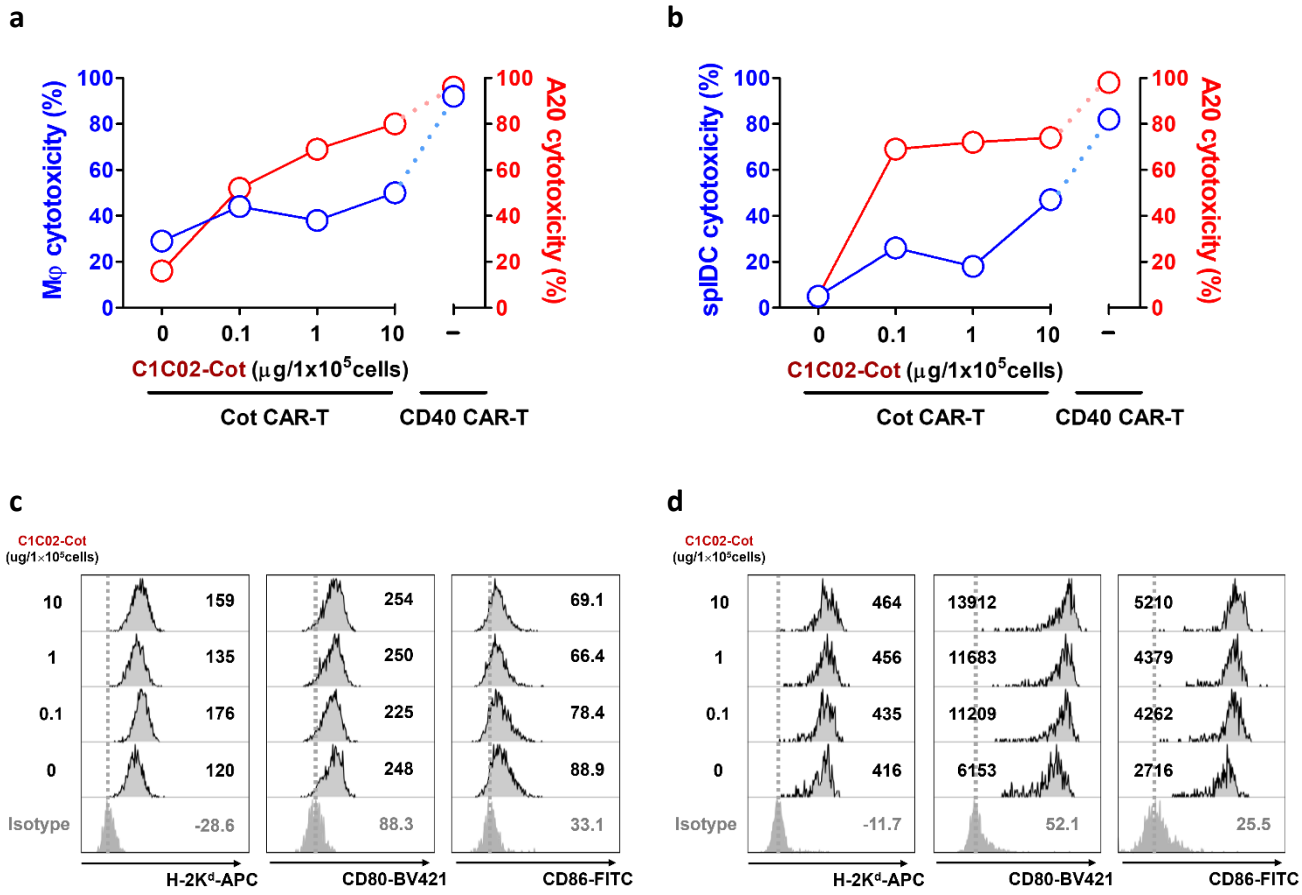

Supplementary Fig. 12 | Cot CAR-T cells with adaptors show much lower cytotoxicity on macrophages and dendritic cells than CD40 CAR-T cells and partially activate dendritic cells. a, b To compare the cytotoxicity of CD40 CAR-T and Cot CAR-T cells, PKH26-labeled macrophages (**a**) or dendritic cells (**b**) and A20 cells (targets) were preincubated with various concentrations of C1C02-Cot and then cocultured with Cot CAR-T cells (effector) at an E:T ratio of 5:1 for 6 hours. CD40 CAR-T cells were co-cultured with target cells not treated with C1C02-Cot. Percent cytotoxicity was calculated from flow cytometric viable cell counts (macrophage cytotoxicity; left axis and blue lines (**a**), dendritic cell cytotoxicity; left axis and blue lines (**b**), and A20 cytotoxicity; right axis and red lines (**a, b**)). Results are representative of at least two independent experiments. **c, d** To test the activation of macrophages or dendritic cells by CD40 CAR-T or Cot CAR-T plus CD40 adaptor, macrophages (**c**) or dendritic cells (**d**) (responders) were preincubated with various concentrations of C1C02-Cot and then co-cultured with CD40 CAR-T or Cot CAR-T cells (stimulators) at a responder: stimulator ratio of 5:1 for 24 hours. Expression of MHC (H-2K^d) and costimulatory molecules (CD80 and CD86) on macrophages (**c**) or dendritic cells (**d**) was measured by staining with fluorescence-labeled antibodies. Results are representative of two independent experiments. Source data are provided in the Source Data file.

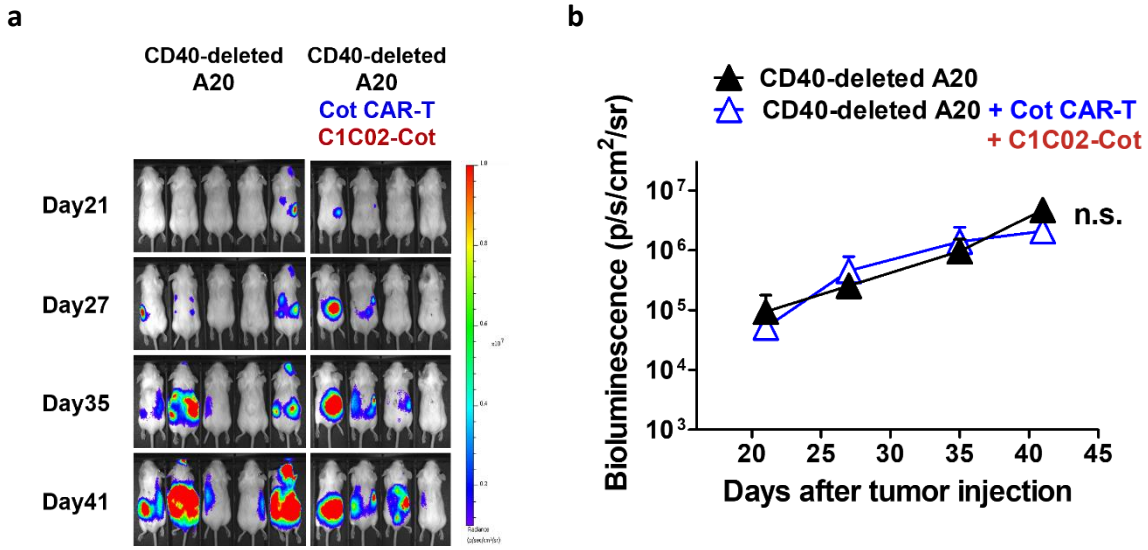

Supplementary Fig. 13 | CD40 expression on tumors is necessary for the antitumor effect of CD40 CAR-T cells. Balb/C mice were injected *i.v.* with CD40-deleted A20-Luc cells (1×10^6) on day 0, irradiated (2.5 Gy) for lymphodepletion on day 6, and injected with Cot CAR-T cells (5×10^6) on day 7. From the day of CAR-T cell injection, C1C02-Cot (20 μg/head) was injected *i.v*. every other day for a total of 8 times. **a** Bioluminescence imaging of tumor burden after Cot CAR-T cell plus C1C02-Cot treatment at indicated time points after tumor cell injection. **b** Bioluminescence intensity was calculated as the mean flux (p/s/cm^2/sr) of a region of interest (ROI) in an individual mouse (*n*=4 or 5). Data are presented as mean ± SEM and statistical significance was determined by unpaired two-tailed *t*-test at each time point (n.s.: not significant). Results are representative of two independent experiments. Source data are provided in the Source Data file.

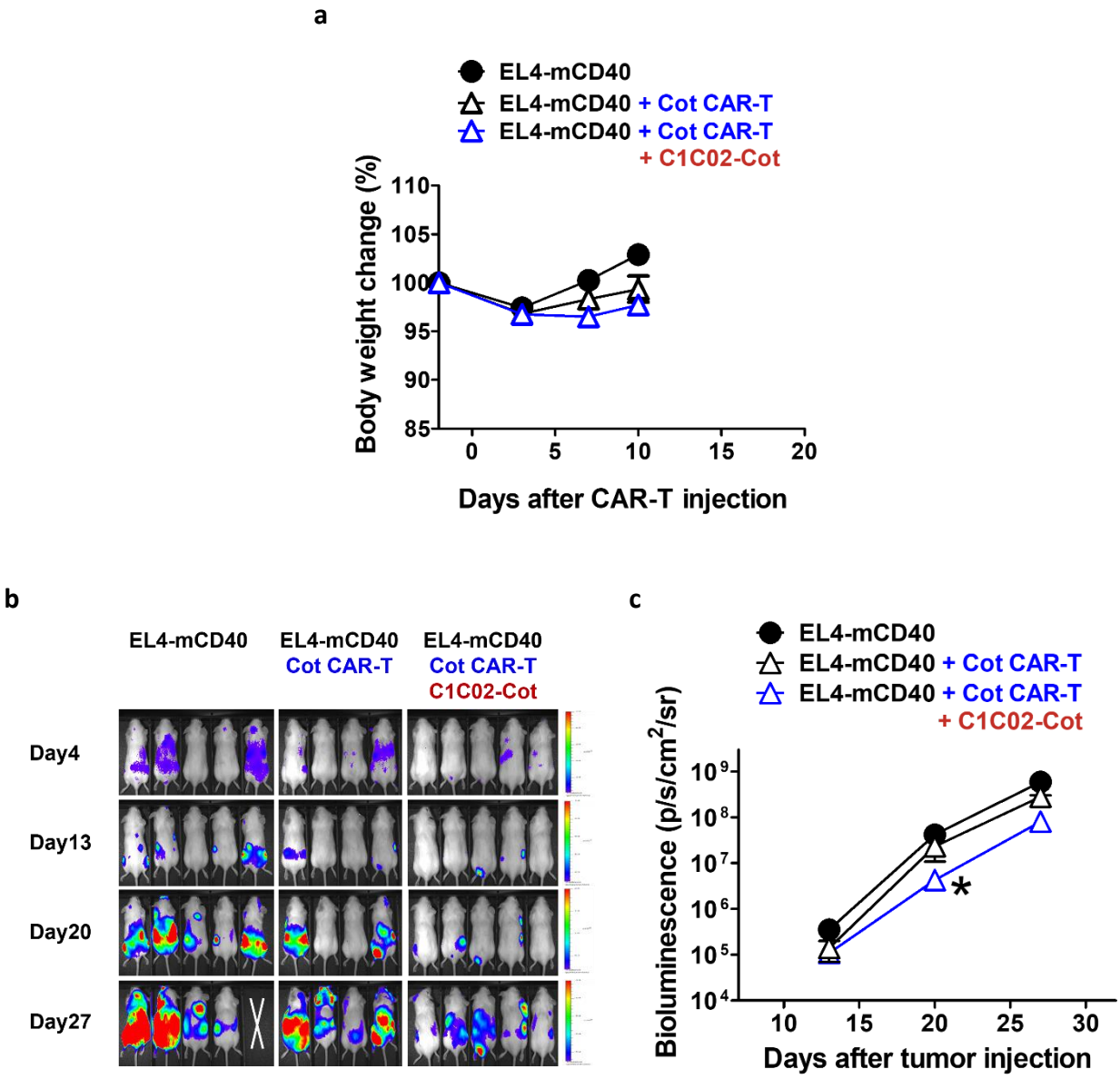

Supplementary Fig. 14 | Cot CAR-T cells with CD40 adaptors show partial therapeutic efficacy in B6 mice. Albino B6 mice were injected *i.v.* with EL4-mCD40-Luc cells (5×10^5) on day 0, irradiated (3 Gy) for lymphodepletion on day 6, and injected with Cot CAR-T cells (5×10^6) on day 7. From the day of CAR-T cell injection, C1C02-Cot (20 μg/head) was injected *i.v.* every other day for a total of 8 times. **a** Body weight changes (n=5) were measured. **b** Bioluminescence imaging of tumor burden after Cot CAR-T cell plus C1C02-Cot treatment at indicated time points after EL4-mCD40-Luc cell injection. **c** Bioluminescence intensity was calculated as the mean flux (p/s/cm^2/sr) of a region of interest (ROI) in an individual mouse (n=4 or 5). Data are presented as mean ± SEM (**a, c**) and statistical significance between groups at each time point was determined by the nonparametric Kruskal-Wallis test (**c**). *: p<0.05, compared to EL4-mCD40 only group. Results are representative of two independent experiments. p: p-value. Source data are provided in the Source Data file.

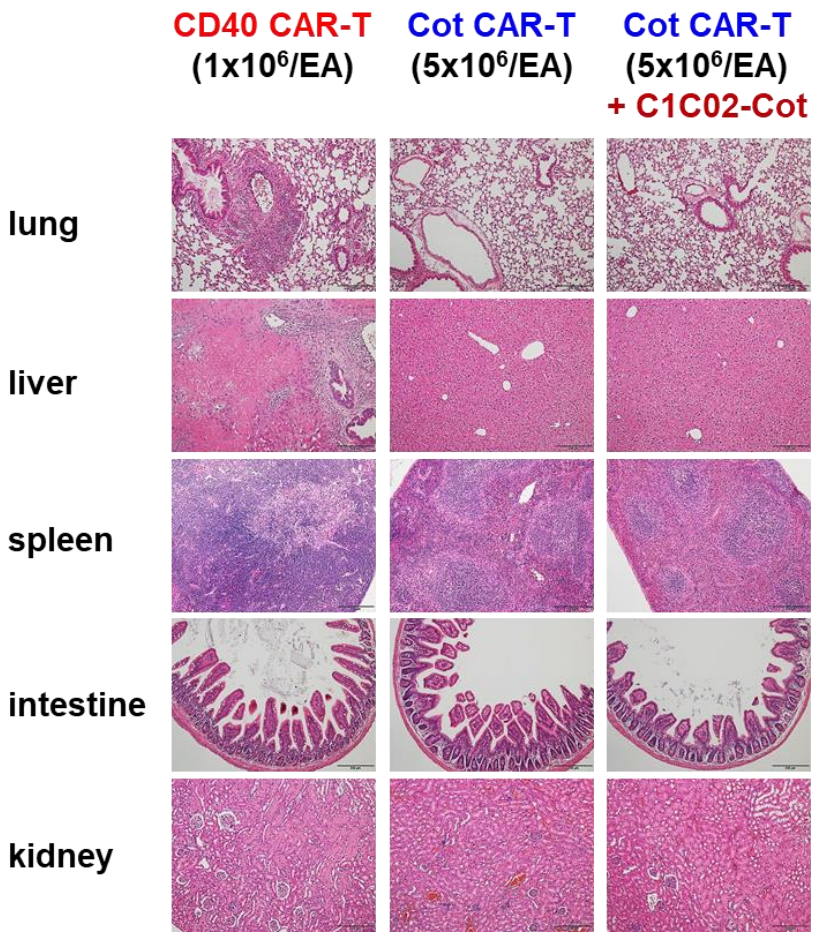

Supplementary Fig. 15 | Cot CAR-T cells with CD40 adaptors do not cause normal tissue inflammation. Balb/C mice implanted with subcutaneous A20 tumor were irradiated (2.5 Gy) for lymphodepletion on day -1 and injected with CD40 CAR-T cells (1×10^6) or Cot CAR-T cells (5×10^6) on day 0. C1C02-Cot (20 μg/head) was injected intravenously every other day from day 0. After 10 days of CAR-T cell injection, various organs were isolated and fixed. The paraffin-embedded tissues were sectioned and stained with H&E. In CD40 CAR-T cell-treated mice, acute vasculitis in the lung was noted. Large vessels were more affected than small vessels. In the liver, infarction characterized by massive parenchymal necrosis and portal vein embolism were observed. In the spleen, necrotic areas with thromboembolic vessels were observed. There were minimal to no abnormal lesions in the intestine and kidney. In Cot CAR-T cell-treated mice and mice treated with Cot CAR-T cells plus C1C02-Cot, there were no abnormalities in all organs examined, including lung, liver, spleen, intestine, and kidney (100× magnification, scale bar: 200 μm). Results are representative of two independent experiments.

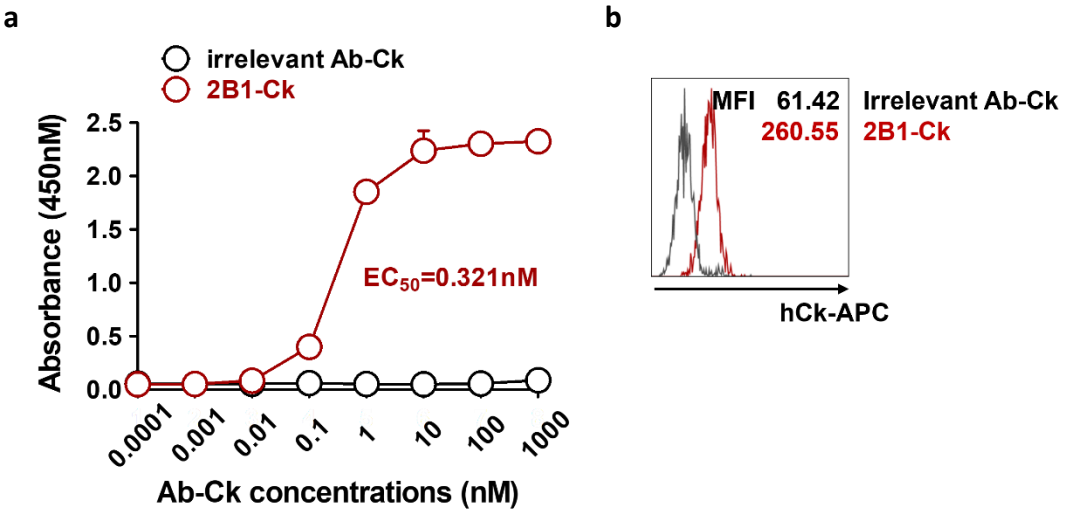

Supplementary Fig. 16 | The anti-human CD40 antibody (clone 2B1) binds to both recombinant human CD40 protein and cell surface CD40 on human Daudi lymphoma cells. a Recombinant human CD40-Fc (2.5 μg/ml) was coated on an ELISA plate, and serial dilutions of 2B1-Cκ or irrelevant scFv antibody-Cκ were loaded. Bound scFv-Cκs were detected by secondary anti-human Cκ-HRP followed by chromogenic reaction with TMB substrate, measured in duplicate. Absorbance was measured at 450 nm. The EC_{50} of antibody binding was calculated as the dose that showed 50% absorbance of maximal binding. Data are presented as mean ± SEM. Results are representative of two independent experiments. **b** Daudi, a CD40-expressing human B-cell lymphoma cells were stained with 2B1-Cκ or irrelevant scFv-Cκ (1 μg/1x10^5 cells) followed by secondary anti-human Cκ-APC. Binding intensity of scFv-Cκs was analyzed by flow cytometry. Numbers are mean fluorescence intensities (MFIs) of binding. Results are representative of three independent experiments. Source data are provided in the Source Data file.

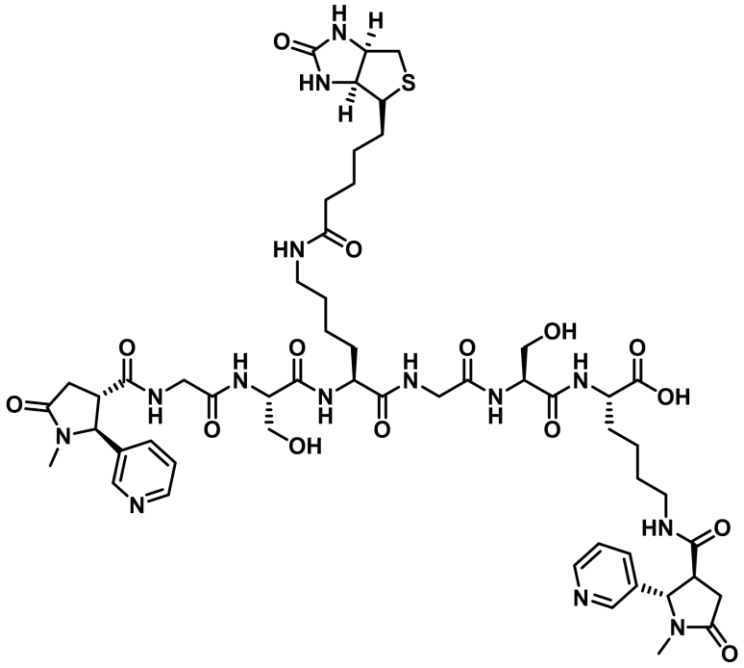

Supplementary Fig. 17 | Chemical structure of biotin-conjugated cotinine. Two cotinine molecules were linked to one biotin using a hexapeptide (GSKGSK) linker by chemical synthesis (cotinine-Gly-Ser-Lys-(biotin)-Gly-Ser-Lys-cotinine) and used as biotin-conjugated cotinine.

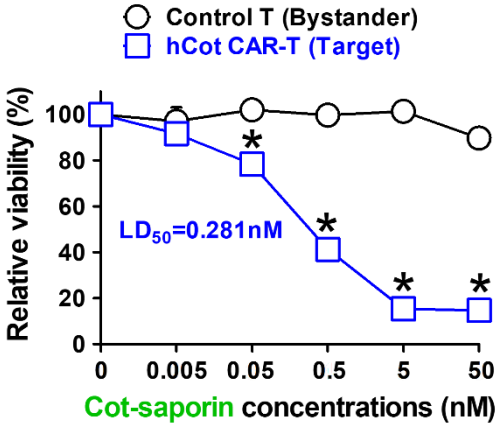

Supplementary Fig. 18 | hCot CAR-T cells can also be selectively killed *in vitro* by cotinine-drug conjugate. PKH26-labeled control T cells (bystander) and unlabeled hCot CAR-T cells (target) were mixed in a 1:1 ratio and incubated with serial dilutions of Cot-saporin. After incubation for 48 hours in medium containing IL-2, viable bystander and target cells were counted by flow cytometry-based viable cell counting. LD_{50}, the dose at which Cot-saporin is lethal for 50% of hCot CAR-T cells. Data are presented as mean ± SEM and statistical significance was determined by unpaired two-tailed *t*-test (*n*=3). *: $p<0.0001$ at 0.05 nM, 0.5 nM, 5 nM, and 50 nM. Results are representative of two independent experiments. Source data are provided in the Source Data file.

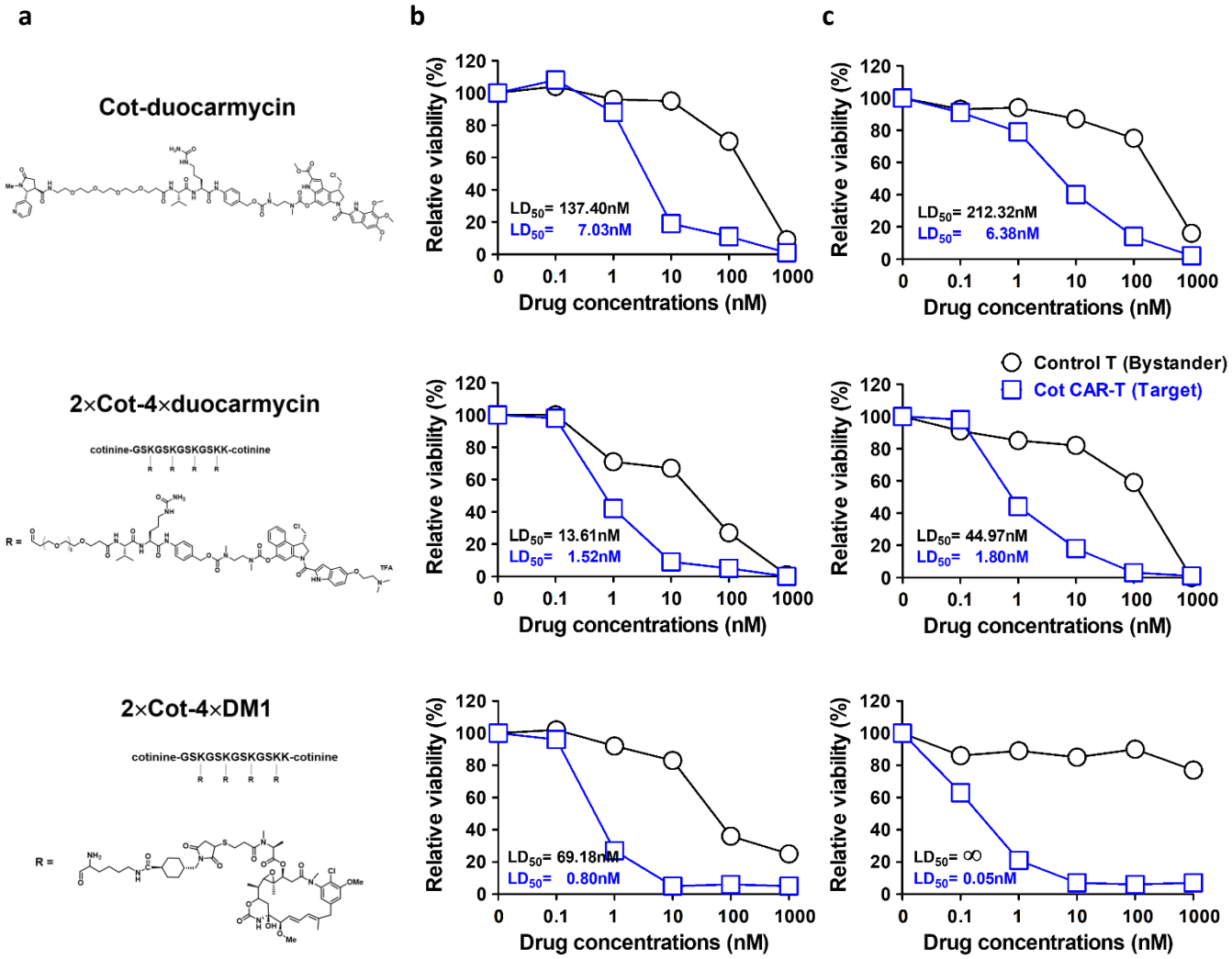

Supplementary Fig. 19 | *In vitro* toxicity of cotinine-conjugated small molecule toxins (duocarmycin or emtansine (DM-1)) on murine and human Cot CAR-T cells. a Chemical structures of cotinine-conjugated small molecule toxins: Cot-duocarmycin; trans-4-Cot-PEG4-vc-PAB-ducoramycin SA (top), 2xCot-4xduocarmycin; [Cot-GSKGSKGSKGSKK-Cot](PEG-vc-PAB-DMAE-duocarmycin SA)$_4$ (middle), and 2xCot-4x-DM1; [Cot-GSKGSKGSKGSKK-Cot](Lys-MCC-DM1)$_4$ (bottom). **b, c** *In vitro* toxicity of cotinine-conjugated drugs on murine Cot CAR-T cells (**b**) and human Cot CAR-T cells (**c**). PKH26-labeled control T cells (bystander) and unlabeled Cot CAR-T cells (target) were mixed in a 1:1 ratio and incubated with serial dilutions of cotinine-conjugated small molecule toxins. After 48 hours in medium containing IL-2, viable bystander and target cells were counted by flow cytometry-based viable cell counting. LD_{50}, the dose at which cotinine-conjugated toxins were lethal for 50% of Cot CAR-T cells. Results are representative of two independent experiments. Source data are provided in the Source Data file.

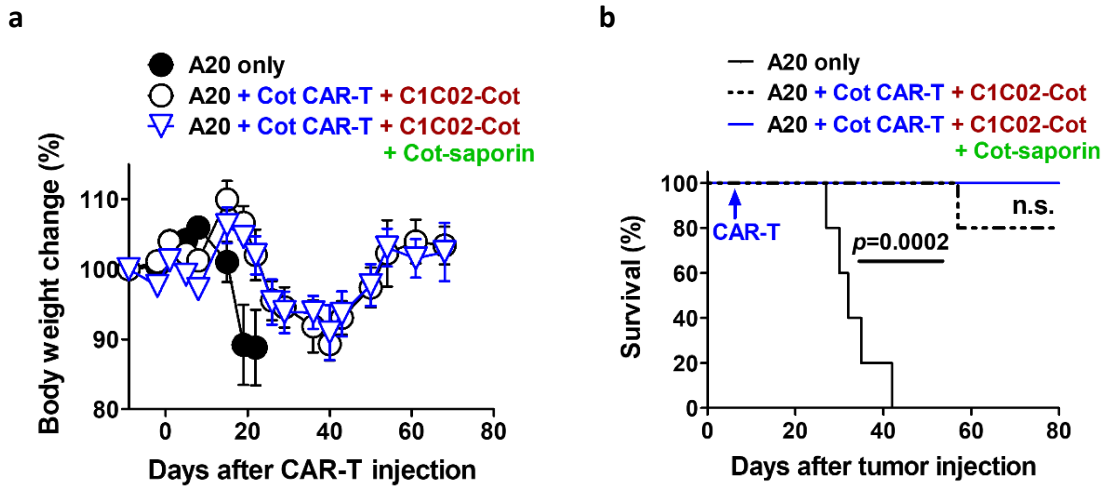

Supplementary Fig. 20 | Cot-saporin treatment does not induce additional toxicity from the saporin drug itself. Body weight change (**a**) and survival (**b**) were measured after B6 Cot CAR-T cell injection into A20 tumor-bearing CB6F1 mice pre-transplanted with B6 bone marrow cells (*n*=5). Cot-Saporin was administered on days 31, 34, and 37 after CAR T-cell injection to control GVHD. Body weight measurements for the tumor alone group were halted when mice began to die (red asterisks in **a**). Data are presented as mean ± SEM (**a**) and statistical significance for survival was determined by log-rank (Mantel-Cox) test (**b**). n.s., not significant. Results are representative of two independent experiments. *p*: p-value. Source data are provided in the Source Data file.

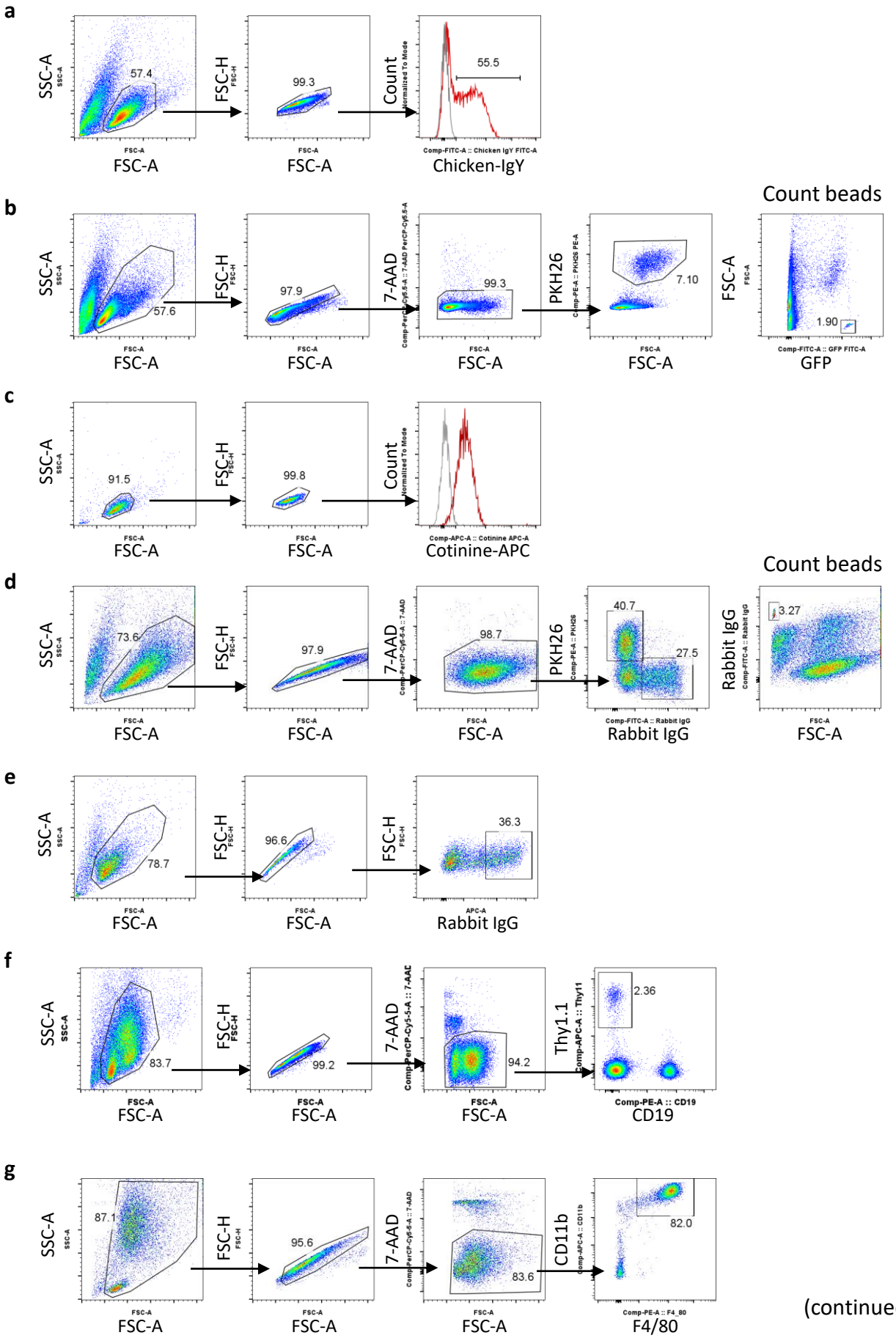
a
SSC-A
FSC-A
57.4
FSC-H
FSC-A
99.3
Count
Chicken-IgY
55.5
b
SSC-A
FSC-A
57.6
FSC-H
FSC-A
97.9
7-AAD
FSC-A
99.3
PKH26
FSC-A
7.10
Count beads
FSC-A
GFP
1.90
c
SSC-A
FSC-A
91.5
FSC-H
FSC-A
99.8
Count
Cotinine-APC
d
SSC-A
FSC-A
73.6
FSC-H
FSC-A
97.9
7-AAD
FSC-A
98.7
PKH26
Rabbit IgG
40.7
27.5
Count beads
Rabbit IgG
FSC-A
3.27
e
SSC-A
FSC-A
78.7
FSC-H
FSC-A
96.6
FSC-H
Rabbit IgG
36.3
f
SSC-A
FSC-A
83.7
FSC-H
FSC-A
99.2
7-AAD
FSC-A
94.2
Thy1.1
CD19
2.36
g
SSC-A
FSC-A
87.1
FSC-H
FSC-A
95.6
7-AAD
FSC-A
83.6
CD11b
F4/80
82.0

(continued)

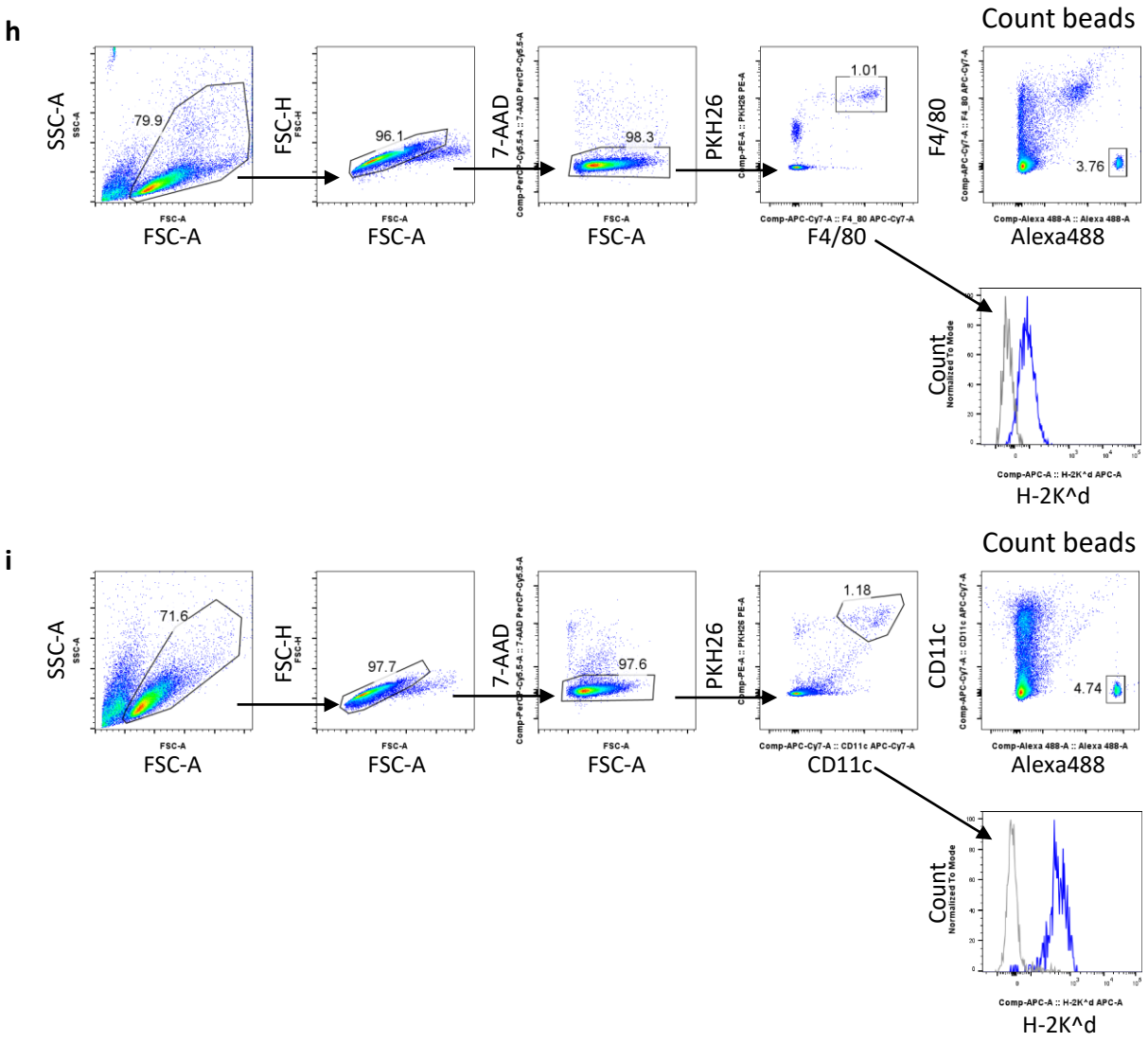

Supplementary Fig. 21 | Gating strategies used for flow cytometry analysis and cell sorting. a Gating strategy to analyze CAR expression on T cells presented in Fig. 1b, 3b and 5b. **b** Gating strategy to analyze target cell (7-AAD-PKH26+) viability in the *in vitro* CAR-T cell cytotoxicity assay presented in Fig. 1c, 3d and 5c and Supplementary Fig. 10c and 10d. **c** Gating strategy to analyze adaptor binding and CD40 expression on target cells presented in Fig. 3c, 3f-h and 5b and Supplementary Fig. 1b, 10b and 16b. **d** Gating strategy to analyze bystander T cell (7-AAD-PKH26+) viability and Cot CAR-T cell (7-AAD-rabbit IgG+) viability in the *in vitro* toxicity of Cot-saporin on Cot CAR-T cells presented in Fig. 6c and Supplementary Fig. 18 and 19. **e** Gating strategy to sort Cot CAR-T cells (rabbit IgG+) (generated from T cells in Thy1.1 mice) used for *in vivo* depletion of Cot CAR-T cells by Cot-saporin treatment in Fig. 6d. **f** Gating strategy to analyze *in vivo* viable Cot CAR-T cells (7-AAD-Thy1.1+) from Cot-saporin treated mice presented in Fig. 6e, 6f, 7d and 7e. **g** Gating strategy to verify *in vivo* depletion of macrophages (F4/80+CD11b+) in mouse peritoneal lavage fluids used in clodronate treatment experiments presented in Fig. 2c-f and Supplementary Fig. 6. **h, i** Gating strategy to analyze macrophage (**h**, 7-AAD-PKH26+F4/80+) or dendritic cell (**i**, 7-AAD-PKH26+CD11c+) viability in the *in vitro* CAR-T cell cytotoxicity assay presented in Supplementary Fig. 12a and 12b, and to analyze expression of MHC (H-2K^d) and co-stimulatory molecules (CD80 and CD86) on macrophages and dendritic cells presented in Supplementary Fig. 12c and 12d. Cell-counting beads for FACS-based cell counting were analyzed in ungated plots (**b, d, h, i**).